P2.32   **SENSITIVITY OF PRECIPITATION FORECAST**
TO THE RADIATIVE IMPACT OF SAHARAN DUST DURING COPS

J.-P. Chaboureau[1], E. Richard[1], J.-P. Pinty[1], C. Flamant[2], P. Di Girolamo[3],
C. Kiemle[4], A. Behrendt[5], H. Chepfer[6], M. Chiriaco[2], and V. Wulfmeyer[5]

[1]Laboratoire d'Aérologie, University of Toulouse and CNRS, France
[2]LATMOS, Université Pierre et Marie Curie and CNRS, Paris, France
[3]DIFA, Università degli Studi della Basilicata, Potenza, Italy
[4]IPA, DLR, Oberpfaffenhofen, Germany
[5]IPM, Universität Hohenheim, Stuttgart, Germany
[6]LMD, IPSL, Université Pierre et Marie Curie, Paris, France

1. INTRODUCTION

From June to August 2007, the international field campaign called the Convective and Orographically-induced Precipitation Study (COPS) took place in south-western Germany and eastern France. The goal of COPS was to advance the quality of forecasts of orographically-induced convective precipitation by four-dimensional observations and modeling of its life cycle. Here, we focus on a line of thunderstorms that triggered on the afternoon of 1st August 2007 over southwestern France. Prior to this convective episode, several ground-based lidars observed a dust layer reaching the COPS area. The dust layer was also seen from airborne lidars in both the COPS area and upstream, over the Iberian Peninsula and France. Some days before, Cloud-Aerosol Lidar and Infrared Pathfinder Satellite Observation observations probed the dust layer off the Moroccan coasts. The long-range transport of this dust event was investigated using a mesoscale model Meso-NH. For evaluation purposes, a lidar simulator was developed by adopting the so-called model-to-satellite approach following Chaboureau et al. (2008, and references therein).

2. MODEL AND LIDAR OBSERVATIONS

The numerical simulations were performed with the non-hydrostatic mesoscale model Meso-NH (Lafore et al. 1998) version 4.7. The two-way interactive grid-nesting method enabled the model to be run simultaneously on several domains with the same vertical levels but with different horizontal resolutions. The lateral boundary conditions were given by large-scale European Centre for Medium-Range Weather Forecasts (ECMWF) operational analyses for the outermost model, and they were provided by the outer models for the inner models at every time step. The case was simulated with triply nested models, with a horizontal grid spacing of 32, 8, and 2 km.

For the two coarser-resolution grids (32 and 8 km), the subgrid-scale convection was parameterized by a mass-flux convection scheme (Bechtold et al. 2001). For the inner grid (2 km), explicit deep convection was permitted and the convection scheme was switched off. The microphysical scheme included the three water phases with five species of precipitating and non-precipitating liquid and solid water (Pinty and Jabouille 1998) and a modified ice to snow autoconversion parameterization following Chaboureau and Pinty (2006). Subgrid cloud cover and condensate content were parameterized as a function of the normalized saturation deficit by taking both turbulent and convective contributions into account (Chaboureau and Bechtold, 2002, 2005). The turbulence parameterization was based on a 1.5-order closure. The surface energy exchanges are represented according to the four possible surface-type patches (nature land surfaces, urban areas, ocean, lake) included in a grid mesh. The Interactions between Soil, Biosphere and Atmosphere (ISBA) scheme was used for natural land surfaces. The radiative scheme was the one used at ECMWF.

The dust prognostic scheme is described in Grini et al. (2006). In this parameterization, the three lognormal modes are generated and transported by the lognormal aerosol scheme of the ORganic and Inorganic Log-normal Aerosols Model (ORILAM). These modes

are described by their 0th, 3rd and 6th moments, with the latter kept constant. Dust fluxes are calculated from wind friction speeds using the Dust Entrainment and Deposition (DEAD) model. The initial dust size distribution contains three modes with median radii of 0.32, 1.73 and 4.33 µm and standard deviations of 1.7, 1.6 and 1.5, respectively. Dust loss occurs through sedimentation and rain out in convective clouds. Regarding the shortwave effect, a refractive index of the dust aerosols was assigned according to that measured over West Africa.

3. TRANSPORT OF SAHARAN DUST TO EUROPE

3.1 *Saharan dust reaching France*

Embedded in low-level south-westerlies, the dust layer reached the Iberian Peninsula and western France on 1st August (Figure 1a). An easterly branch expanded over the Atlantic Ocean west of 30°W. Over Africa, the AI remained high, pointing out the persistence of the dust emission. Northerlies over the North African coasts turning to easterlies over the Sahara were still prevalent (Figure 1b). The simulated dust burden showed several similarities with the retrieved AI, in terms of both structure and amplitude. A smaller dust burden was simulated in the south-eastern corner due to the proximity of the domain border. Lower values were also found over Southern Algeria, which can be explained by the lack of dust transported over a range longer than the simulation domain. On the other hand, the western extent of dust over the Atlantic Ocean looked correct, as did the dust load that spread up to western France. This spread in dust over France was confirmed by the comparison with the DLR observations as discussed in the following.

The DLR Falcon flew over the south-westerly flow between Faro, Portugal, and Oberpfaffenhofen, Germany, as this area was targeted as a sensitive region for quantitative precipitation forecast over the COPS region. The vertical cross section of the attenuated backscattered (ATB) signal at 1064 nm is shown in Figure 2. Consistently with the OMI retrievals, the

dust layer extended up to 45°N. This layer was relatively moist, with a water vapor mixing ratio larger than 2 g/kg, compared to the dry conditions prevailing further north. Isolated maxima of backscattered signal at 6-km altitude also indicated the presence of clouds on the top of the dust layer. Below the leading edge of the dust layer, a tongue of dry air could be seen at 2-km altitude. The origin of this layer is identified in the following as subsiding air from the midtroposphere.
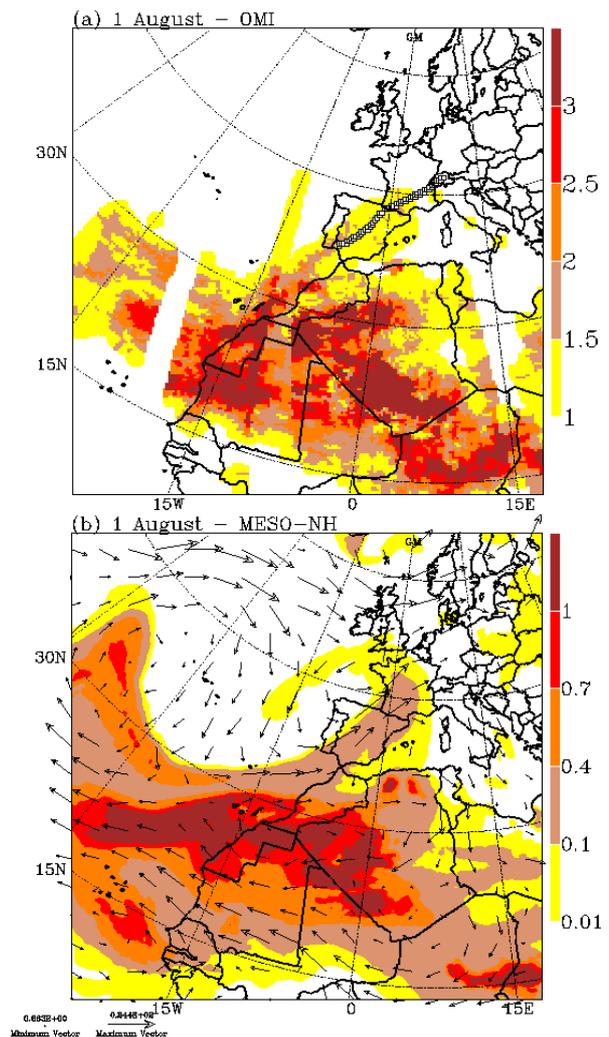

Fig. 1. (a) OMI aerosol index and (b) Meso-NH total aerosol burden (g/m^2) at 1200 UTC 1 August 2007. In (b) the arrows show the 700-hPa wind vectors from Meso-NH. In (a) the line of squares indicates the track of the DLR Falcon. The domain is 6400-km long. Longitude and latitude lines are plotted every 15°.
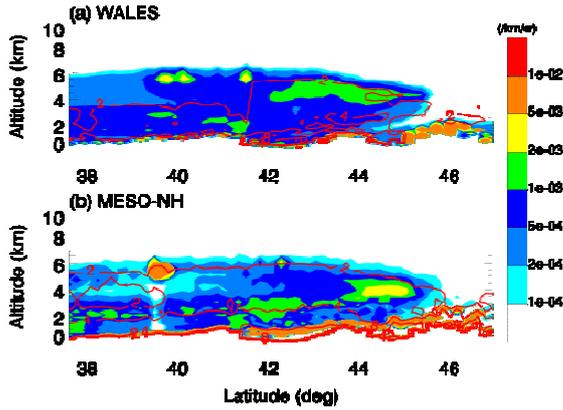
Fig.2 Vertical cross-section of ATB signal at 1064 nm (shading, /km/sr) and water vapour mixing ratio (contours at 2, 4, 8 g/kg) on 1 August 2007 along the line shown in Figure 1b from (a) WALES between 0900 and 1100 UTC and (b) Meso-NH at 1200 UTC.

3.2 *Arrival of dust over Achern*

At 1700 UTC on 1st August, the dust layer arrived over the COPS area as observed by the BASIL Raman lidar operating at Achern, Germany (Figure 3a). The PBL, with a thickness of about 1.5 km, was characterized by a mixing ratio higher than 4 g/kg and a particle backscatter coefficient β_{par} larger than $2\ 10^{-4}$. Due to its location in the PBL, this coefficient could be identified as representative of background aerosol. At 2000 UTC, the depth of the layer with mixing ratio larger than 8 g/kg increased while β_{par} decreased, suggesting a change in airmass. A first change in airmass occurred just above 1.5 km at 1600 UTC with the arrival of dry air with mixing ratio values smaller than 2 g/kg. At 1800 UTC this airmass was replaced by a dusty one above 2 km while the dry layer remained beneath. Consistently with the LEANDRE 2 observation, the dust layer could be divided into two sub-layers. The one located between 3 and 5 km gave more backscattering than the layer below, the latter being moister, with a water vapour mixing ratio larger than 4 g/kg.
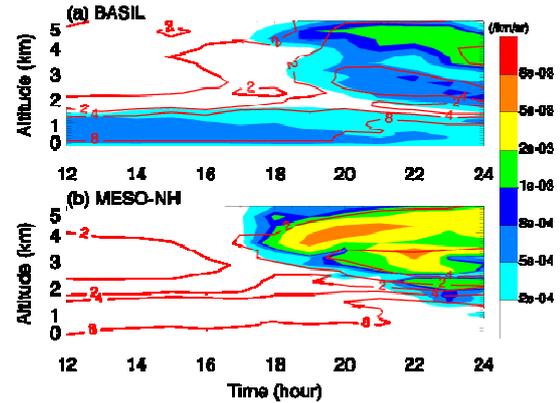

Fig. 3: Time series of β_{par} at 1064 nm (shading, /km/sr) and water vapor mixing ratio (contours at 2, 4, 8 g/kg) over Achern from 1200 UTC 1 August to 0000 UTC 2 August 2007 for (a) BASIL and (b) Meso-NH.

The Meso-NH simulation shows good agreement with the observations in capturing the height and arrival time of the dust layer (Figure 3b). However, the dust layer lacks the fine-scale structure sensed by BASIL, showing a dust contribution to the lidar signal spanning too thick a layer. Note also the absence of lidar signal in the first km due to the lack of background aerosols in the simulation. On the other hand, the simulated water vapour mixing ratio is in agreement with the BASIL measurements. For example, the increase in water vapour at 2000 UTC is simulated in the first km, as is the arrival of the dry layer first in the free troposphere then just above the PBL. This is also true for the pocket of enhanced water vapour values over 4 g/kg found around 3 km. These results give us confidence in the simulated transport of airmasses.

In order to check the origin of air masses, backward trajectories were computed. Parcels in the same vertical column over Achern were taken at 1, 2, 3, and 4 km altitudes and their origins 6 days earlier were determined (Figure 4). Parcels at 4-km altitude show backward trajectories that follow the pathways of the dust burden seen in Figure 1b. This clearly confirms the origin of dust as northern Africa. Parcels at 3-km altitude can be traced back to the PBL over the Atlantic Ocean. This result agrees well with the spectral analyses of the BASIL observations. Using information

provided by the BASIL measurements at three wavelengths, the layer content was identified as a mixture of dust and sea salt. Parcels at 2-km altitude were characterized by clean and relatively dry air. On 28th July, the parcels subsided from 4 to 1.5 km over the Atlantic ocean. Their midtropospheric origin explains the low water vapour content, around 2 g/kg, well. Finally, parcels at 1-km altitude came from the Rhone valley two days earlier. In the valley, there are many cities, industrial plants, and motorways. These anthropogenic sources explain the large background aerosol content measured by BASIL. This signal was missed by Meso-NH as no urban aerosol was simulated.
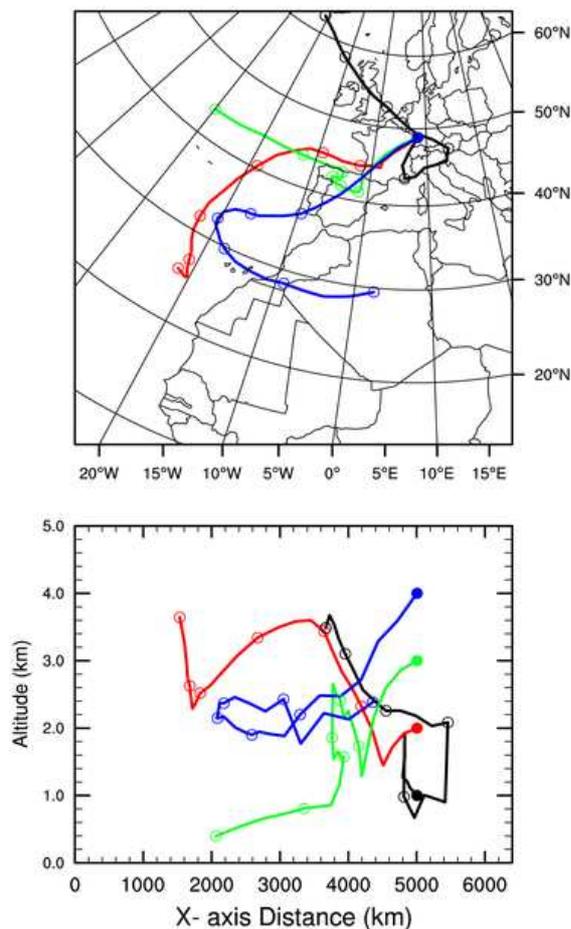

Fig. 4. Backward trajectories from 0000 UTC 27 July 2007 to 0000 UTC 2 August 2007. (b) represents a projection of the trajectories along the x-axis of the simulation domain. Circles on the backward trajectories are spaced at 24-h intervals, the filled circles show the starting points.

3. IMPACT OF DUST ON RAIN FORECAST

The sensitivity of the precipitation forecast to the radiative impact of the dust layer was investigated using three simulations: DUST using the dust prognostic scheme, CLIM using a climatology of dust as applied in some operational numerical weather prediction models, and NODUST, which does not consider any dust effect. Only the radiative effect of dust was considered here. No interaction between dust aerosols and clouds was taken into account. Simulations were run over 5 days to allow the dust to have a sufficient radiative impact on the thermodynamic structure of the atmosphere.
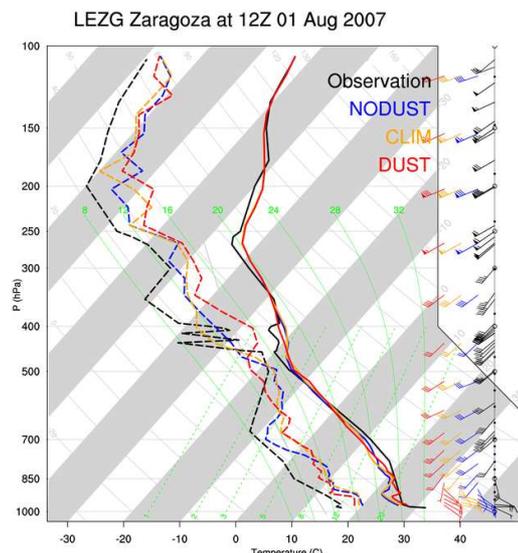

Fig. 5. Skew-T diagramme over Zaragoza, Spain at 1200 UTC 1 August 2007 for observation (thick line) and simulations (thin lines).

The differences in temperature between DUST and the other two experiments were limited to small values, around 2 K, and below the 6-km altitude as imposed in the simulation setup. These small changes appeared to be always positive when compared with radiosonde data at 1200 UTC on 1st August. Among the stations examined over Spain and France, the example with the largest change was Zaragoza, Spain (41.66°N, 1.01°W; Figure 5). From ground level to 750 hPa, i.e. within the dust layer, the temperature was enhanced by a few K in

DUST compared to NODUST and CLIM. The largest increase, 3.4 K, occurred at 910 hPa (830-m altitude). In particular, this increase made the DUST temperature profile closer to the observed one.

These small changes in temperature, this in static stability, have an impact on the resulting rain shown with 6-hour accumulated precipitation valid at 0000 UTC 2 August 2007. The ability of the simulations to forecast the rain event at the right place was quantified with the Equitable Threat Score (ETS). ETS measures the correspondence between simulated and observed occurrence of events at grid points. It was calculated for the 6-h accumulated rain at 0000 UTC on 2nd August over the inner domain (Figure 6). From the 1-mm category and for each simulation, the ETS decreased as the threshold increased. Higher ETS were found for DUST whatever the rain category. This result shows that a better rain forecast was provided, for this particular event, by the simulation using a dust prognostic scheme.
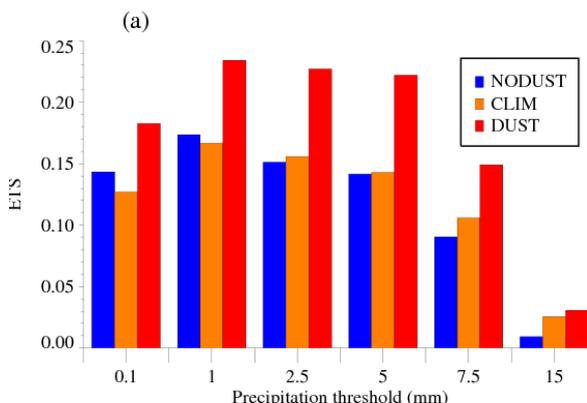

Fig. 6. Equitable Threat Score (ETS) for (a) 6-h accumulated precipitation (mm) at 0000 UTC 2 August 2007.

4. CONCLUSION

A Saharan dust event affected the Rhine valley on 1st August 2007 during the COPS experiment prior to a convective event. This case was investigated using lidar observations from space, aircraft and ground, and a regional model. The consistency between the different sets of information allowed the sources of dust to be identified. Both observations and simulation supported the fact that dust at 4-km altitude originated from the Sahara 6 days earlier. In addition, dry air was observed at 2-km altitude by the different water vapor lidar systems operating over France and Germany. The agreement with the simulation allowed the dry air to be traced back as subsiding 5 days before from the midtroposphere over the Atlantic Ocean. This consistency between observations and simulation gives us further confidence in the identification of the aerosol observed at 3-km altitude over Achern as a mixture of dust and sea salt.

The direct comparison between observed and simulated backscattered signals shows the good performance of the model in terms of characterization and transport of dust. The lidar simulator developed here is shown to be a powerful tool for evaluation following the model to satellite approach employed by Wiedner et al. (2004), Meirold-Mautner et al. (2007), and Söhne et al. (2008), among others. This simulator will be used for many other applications. Its use is foreseen for the evaluation of case studies such as those observed during the African Monsoon Multidisciplinary Analysis (AMMA) campaign (e.g. Flamant et al. 2009) and from which an estimate of dust emission was made (e.g. Bou Karam et al. 2009). The simulator still needs further development to take account of the nonspherical shape of cirrus crystals that will be modeled by a sophisticated microphysics cloud scheme.

The radiative impact of dust on precipitation forecasts was also investigated. Three simulations, with or without the dust prognostic scheme or using a dust climatology were run forward for 5 days. The radiative effect of dust generated some perturbations in temperature. The latter resulted in a change in static stability. Here, the enhancement of dust over France led to a decrease in static stability along the thunderstorm path. In consequence, precipitation showed better agreement with rain gauges as assessed with the skill score. This suggests that skill in rain forecasts could be increased at 5-day range by using a prognostic scheme during dust episodes reaching Europe. More details are given in Chaboureau et al. (2010, manuscript in revision for QJRMS).

5. REFERENCES

Bechtold P, Bazile E, Guichard F, Mascart P, Richard E. 2001: A mass flux convection scheme for regional and global models. *Quart. J. Roy. Meteor. Soc.*, **127**, 869–886

Bou Karam D, Flamant C, Tulet P, Chaboureau JP, Dabas A, Todd MC. 2009: Estimate of Sahelian dust emissions in the inter-tropical discontinuity region of the West African Monsoon. *J. Geophys. Res.*, **114**, D13106, doi:10.1029/2008JD011444.

Chaboureau, J.-P. and P. Bechtold, 2002: A simple cloud parameterization derived from cloud resolving model data: diagnostic and prognostic applications. *J. Atmos. Sci.*, **59**, 2362-2372

Chaboureau, J.-P., and P. Bechtold, 2005: Statistical representation of clouds in a regional model and the impact on the diurnal cycle of convection during Tropical Convection, Cirrus and Nitrogen Oxides (TROCCINOX), *J. Geophys. Res.*, **110**, D17103, doi:10.1029/2004JD005645.

Chaboureau, J.-P., N. Söhne, J.-P. Pinty, I. Meirold-Mautner, E. Defer, C. Prigent, J. R. Pardo, M. Mech, and S. Crewell, 2008: A midlatitude precipitating cloud database validated with satellite observations. *J. App. Meteorol. Clim.*, **47**, 1337–1353.

Chaboureau, J.-P., P. Tulet, and C. Mari, 2007: Diurnal cycle of dust and cirrus over West Africa as seen from Meteosat Second Generation satellite and a regional forecast model. *Geophys. Res. Lett.*, **34**, L02822, doi:10.1029/2006GL027771

Chaboureau, J.-P. and J.-P. Pinty, 2006: Evaluation of a cirrus parameterization with Meteosat Second Generation observations. *Geophys. Res. Let.*, **33**, L03815, doi:10.1029/2005GL024725

Flamant C, Lavaysse C, Todd M, Chaboureau JP, Pelon J. 2009. Multiplatform observations of a representative springtime case of Bodélé and Sudan dust emission, transport and scavenging over West Africa. *Quart. J. Roy. Meteor. Soc.*, **135**, 413–430

Grini A, Tulet P, Gomes L. 2006 : Dusty weather forecasts using the MesoNH mesoscale atmospheric model. *J. Geophys. Res.*, **111**, D19205, doi:10.1029/2005JD007007

Lafore JP, Stein J, Asencio N, Bougeault P, Ducrocq V, Duron J, Fischer C, Héreil P, Mascart P, Masson V, Pinty JP, Redelsperger JL, Richard E, Vilà-Guerau de Arellano J. 1998 : The Meso–NH Atmospheric Simulation System. Part I: adiabatic formulation and control simulations. Scientific objectives and experimental design. *Ann. Geophys.*, **16**, 90–109

Meirold-Mautner, I., C. Prigent, E. Defer, J. R. Pardo, J.-P. Chaboureau, J.-P. Pinty, M. Mech, and S. Crewell, 2007: Radiative transfer simulations using mesoscale cloud model outputs and comparisons with passive microwave and infrared satellite observations for mid-latitude situations. *J. Atmos. Sci.*, **64**, 1550-1568

Pinty JP, Jabouille P. 1998: A mixed-phase cloud parameterization for use in a mesoscale non-hydrostatic model: simulations of a squall line and of orographic precipitations. AMS Conf. on cloud physics, Everett, WA. pp. 217–220

Söhne, N., J.-P. Chaboureau, and F. Guichard, 2008: Verification of cloud cover forecast with satellite observation over West Africa, *Mon. Weather Rev.*, **136**, 4421–4434

Wiedner M, Prigent C, Pardo JR, Nuissier O, Chaboureau JP, Pinty JP, Mascart P. 2004: Modeling of passive microwave responses in convective situations using outputs from mesoscale models: comparison with TRMM/TMI satellite observations. *J. Geophys. Res.*, **109**, D06214, doi:10.1029/2003JD004280